

# Relationship between NogoA/NgR1/RhoA signaling pathway and the apoptosis of cerebral neurons after cerebral infarction in rats

Y.-X. XIE<sup>1</sup>, M. ZHANG<sup>1</sup>, C.-R. ZHANG<sup>2</sup>, F. CHEN<sup>3</sup>

<sup>1</sup>Department of Minimally Invasive Interventional Treatment Center, <sup>2</sup>Department of Outpatient, <sup>3</sup>Department of Neurosurgery; Qingdao Municipal Hospital (Group), Qingdao, China

**Abstract.** – **OBJECTIVE:** The aim of this study was to investigate the effect and the mechanism of the NogoA/NgR1/RhoA signaling pathway on the apoptosis of neurons in cerebral infarction (CI) rats. Our findings might provide references for clinical prevention and treatment of CI.

**MATERIALS AND METHODS:** A total of 60 adult male Wistar rats were randomly divided into 3 groups, including: Sham operation group (Sham group), CI group, and CI + NogoA gene knockout group (CI + NogoA KO group) using a random number table. The model of CI was successfully constructed using suture method in rats of CI group and CI + NogoA KO group. Blood vessels were exposed in Sham group. At 2 days after CI operation, the rats were killed, and brain tissues were collected. Reverse transcription-Polymerase Chain Reaction (RT-PCR) and Western blotting were used to detect the messenger ribonucleic acid (mRNA) and protein expression levels of NogoA/NgR1/RhoA in brain lesion tissues of rats in the three groups, respectively. Subsequently, the infarction area and damage of brain tissues were assessed via hematoxylin and eosin (H&E) staining, TTC staining was carried out to evaluate the infarction area in each group, terminal deoxynucleotidyl transferase dUTP nick end labeling (TUNEL) staining was conducted to measure the apoptosis level of neurons in brain tissues of rats in each group. Additionally, the level of Nissl's body in brain tissues of each group was examined by Nissl staining. Furthermore, the expression level of the platelet-derived growth factor (PDGF) in brain tissues of rats in the three groups was measured via immunohistochemistry.

**RESULTS:** The mRNA and protein expression levels of the NogoA/NgR1/RhoA signaling pathway in brain tissues of rats in CI group increased significantly ( $p < 0.05$ ). NogoA KO group could significantly reduce the infarction area of brain tissues in rats ( $p < 0.05$ ). H&E staining and Nissl's body staining revealed that neurons in the brain tissues of rats showed evident edema and disordered arrangement after CI. Meanwhile, the number of Nissl's body was remarkably reduced. However, after KO of NogoA, brain

tissue damage was significantly alleviated in rats, and the number of Nissl's body increased remarkably at the same time ( $p < 0.05$ ). According to TUNEL staining results, blocking NogoA could notably reduce CI-induced apoptosis of neurons in brain tissues of rats ( $p < 0.05$ ). Immunohistochemical staining results demonstrated that the expression of PDGF in brain tissues of rats in CI group decreased markedly, whereas it was significantly elevated in rats of CI + NogoA KO group ( $p < 0.05$ ).

**CONCLUSION:** The expression of the NogoA/NgR1/RhoA signaling pathway was significantly elevated in brain tissues of CI rats. Furthermore, suppressing the NogoA/NgR1/RhoA signaling pathway could reduce CI-induced apoptosis of neurons in rats.

**Key Words:**

NogoA/NgR1/RhoA, Cerebral infarction (CI), Neuron, Apoptosis.

## Introduction

Cerebral infarction (CI) generally refers to the symptoms of cerebral tissue ischemia, hypoxia, necrosis, neurological dysfunction and even defects caused by an abnormal blood supply in the brain. It is also known as ischemic stroke<sup>1</sup>. Although the current medical technique has developed rapidly, CI is still the main cause of death and disability worldwide<sup>2</sup>. Therefore, it is of great significance to further clarify the occurrence and development of CI for early diagnosis and accurate treatment.

Current studies<sup>3,4</sup> have revealed that varying myelin-related neurite growth inhibitors can suppress the regeneration of damaged axons. For instance, the typical neurite growth inhibitor NogoA is a myelin-derived protein, which can block axonal regeneration and reconnection of damaged axons after stroke<sup>5,6</sup>. NogoA binds to the Nogo receptor

(NgR1) and activates the intracellular RhoGTP enzyme signaling pathway, thereby inducing growth cone collapse<sup>7,8</sup>. Hence, the design of drugs targeting the NogoA/NgR1/RhoA signaling pathway is of great significance for the prevention and treatment of stroke. However, few studies have elucidated the exact role and mechanism of the NogoA/NgR1/RhoA signaling pathway in CI.

In this research, the messenger ribonucleic acids (mRNA) and protein expressions of the NogoA/NgR1/RhoA pathway in infarcted brain tissues of rats with CI were first detected. Moreover, the effects of NogoA knockout (KO) on neuronal apoptosis and pathological damage in the brain tissues of rats were further verified by KO of NogoA.

## Materials and Methods

### Animal Grouping and Model Establishment

Sixty male Wistar rats weighing (85.32±7.61) g at the age of 12-14 weeks old were divided into 3 groups, including: Sham operation group (Sham group), CI group, and CI+NogoA gene KO group (CI+NogoA KO group) using a random number table. The model of CI was successfully constructed using suture method in rats of CI group and CI+NogoA KO group. Meanwhile, only brain vessels were exposed in Sham group. No statistically significant differences were observed in basic data among the three groups, such as weeks of age and body weight. The experimental operation was as follows: 1) Rats were first anesthetized and fixed. 2) The left common carotid artery and vagus nerve were separated. 3) The left common carotid artery and the proximal end of the external carotid artery were ligated, respectively. 4) A thread was prepared from a live knot at the distal end of the left common carotid artery. 5) The left common carotid artery was separated, and an incision was made at the proximal end of the external carotid artery. 6) The bolt was inserted from the incision and pushed forward gradually. When it was pushed forward for about 18 mm, the resistance could be clearly felt. This proved that the head of the bolt reached the middle cerebral artery. 7) After 30 min, the bolt was taken out and reperfusion was carried out. 8) Suture and sterilization were then conducted. After 2 days, scoring was performed, and materials were obtained. This investigation was approved by the Animal Ethics Committee of Qingdao Municipal Hospital (Group) Animal Center.

### Detection of the Expression of Apoptosis-Related Genes Via Reverse Transcription-Polymerase Chain Reaction (RT-PCR)

1) TRIzol assay (Invitrogen, Carlsbad, CA, USA) was used to extract total RNA from brain tissues of rats in each group. The concentration and purity of extracted RNA were measured by an ultraviolet spectrophotometer. When the ratio of absorbance (A)<sub>260</sub>/A<sub>280</sub> was between 1.8 and 2.0, RNA samples could be used. 2) Messenger RNA (mRNAs) were then synthesized into complementary deoxyribonucleic acids (cDNAs) through RT-PCR and stored in a refrigerator at -80°C for use. 3) RT-PCR system was as follows: 2.5 μL Buffer, 2 μL cDNAs, 0.25 μL forward primer (10 μmol/L), 0.25 μL reverse primer (10 μmol/L), 2 μL dNTPs (10 mmol/L), 0.5 μL Taq polymerase (2×10<sup>6</sup> U/L) and 19 μL ddH<sub>2</sub>O. The amplification systems of RT-PCR were the same. The primer sequences used in this work were shown in Table I.

### Detection of Protein Expression Via Western Blotting

Brain tissues of rats in each group were first homogenized in lysis buffer and subjected to ultrasonic fragmentation. After centrifugation, the supernatant was collected and was sequentially sub-packaged into Eppendorf tubes. The concentration of extracted protein samples was measured using the bicinchoninic acid (BCA) assay (Pierce, Rockford, IL, USA) and ultraviolet spectrophotometry. After that, the volume was set constant to the same concentration. After sub-packaging, the samples were placed in a refrigerator at -80°C. The protein samples were separated by sodium dodecyl sulphate-polyacrylamide gel electrophoresis (SDS-PAGE) and transferred onto cellulose acetate (PVDF) membranes (Roche, Basel, Switzerland). After incubation with primary antibodies at 4°C overnight, the membranes were incubated with

Table I. Primer sequences.

Target gene		Primer sequence
GAPDH	Forward	5'-GACATGCCGCTGGAGAAAC-3'
	Reverse	5'-AGCCAGGATGCCCTTAGT-3'
NogoA	Forward	5'-TGCTGCCTTTTCTGTTCCTT-3'
	Reverse	5'-AAGGTGCTGGGTAGGGAAGT-3'
NgR1	Forward	5'-GTCCACGAACCCGTAAGGT-3'
	Reverse	5'-ACGATGCTGGATGCTAGTTCG-3'
RhoA	Forward	5'-ACGTGTGCTAGCCCCACTGATG-3'
	Reverse	5'-CATCTTTTCCCGATAGGTCCA-3'

goat anti-rabbit secondary antibody for 1 h away from light. Immuno-reactive bands were scanned and quantified using an Odyssey membrane sweeper. Glyceraldehyde 3-phosphate dehydrogenase (GAPDH) was used to correct the level of proteins to be tested.

#### **Triphenyl Tetrazolium Chloride (TTC) Staining**

1) Fresh brain tissues were first put into a rat brain tissue slice grinder, followed by frozen in a refrigerator for 30 min at -20°C for slicing. 2) Subsequently, brain tissues were cut into 2 mm-thick slices, with no more than 6 slices per tissue. 3) Prepared slices were then placed in fresh TTC solution (2%) and fully contacted the TTC solution for incubation for no less than 0.5 h. 4) After 0.5 h, the slices were taken out and fixed with 4% paraformaldehyde, followed by photography.

#### **Hematoxylin and Eosin (H&E) Staining**

Brain tissues obtained in each group were first placed in 10% formalin overnight, dehydrated and embedded in paraffin blocks. Subsequently, all brain tissues were cut into slices with a thickness of 5 µm, fixed on glass slides and dried for staining. According to relative instructions, the sections were soaked in xylene, ethanol at gradient concentration and hematoxylin, followed by eosin staining, sealing with resin. After drying in the air, observation and photography were conducted under an optical microscope. Finally, the number of neurons was observed.

#### **Terminal Deoxynucleotidyl Transferase (dUTP) End Labeling (TUNEL) Staining**

Brain tissues were first sliced, baked in an oven at 60°C for 30 min and deparaffinized with xylene (5 min × 3 times). Then, the sections were dehydrated with 100%, 95%, and 70% ethanol, respectively, with 3 times for each. Subsequently, the slices were incubated with protein kinase K for half an hour. After washing with phosphate-buffered saline (PBS), TdT and luciferase-labeled dUTP were added. After reaction for 1 h at 37°C, the sections were incubated with a specific antibody and with horseradish peroxidase at 37°C for 1 h. Next, the sections reacted at room temperature for 10 min, with diaminobenzidine (DAB) as the substrate. After the nucleus was stained with hematoxylin, photography and counting were carried out under an optical microscope.

#### **Immunohistochemical Staining**

Brain tissue slices were first baked in an oven at 60°C for 30 min and deparaffinized with xylene (5 min × 3 times), followed by dehydration with 100%, 95%, and 70% ethanol, respectively, with 3 times for each. Endogenous peroxidase activity was inhibited by 3% hydrogen peroxide solution, and the tissues were sealed with sheep serum for 1 h. Antibodies against platelet-derived growth factor (PDGF) were diluted at 1:200 (PDS) and incubated at 4°C overnight, followed by washing with PBS for 4 times in a shaker. After the sections were incubated with secondary antibody, the color was developed with diaminobenzidine. After color development, 6 samples were randomly selected from each group, and 5 fields of view were randomly selected in each sample. Finally, photographs were performed under an optical microscope (200× and 400×).

#### **Mast Staining**

1) Paraffin-embedded or frozen sections were sequentially stained with xylene, anhydrous ethanol, 95% alcohol, and 70% alcohol, and distilled water. The respective time could be based on H&E staining. 2) The sections were then stained with 1% tar violet and methionine for 10 min to 1 h. 3) Subsequently, the sections were rinsed with distilled water. 4) 70% alcohol color separation was performed for several seconds to several minutes. 5) The sections were dehydrated with 70%, 80%, and 95% alcohol, respectively, with 2 min for each. 6) Next, the sections were washed with anhydrous ethanol twice (with 5 min for each time), followed by washing with xylene twice (with 10 min for each time). 7) Finally, the sections were mounted with DPX.

#### **Statistical Analysis**

Statistical Product and Service Solutions 22.0 software (IBM, Armonk, NY, USA) was used for all statistical analysis. Measurement data were expressed as mean ± standard deviation. The *t*-test was used to compare the difference between the two groups. *p*<0.05 was considered statistically significant.

## **Results**

#### **MRNA Expression of the NogoA/ NgR1/RhoA Signaling Pathway in Brain Tissues of Rats in Each Group**

According to RT-PCR results (Figure 1), the mRNA expressions of NogoA, NgR1, and RhoA in brain tissues of rats in CI group were signifi-

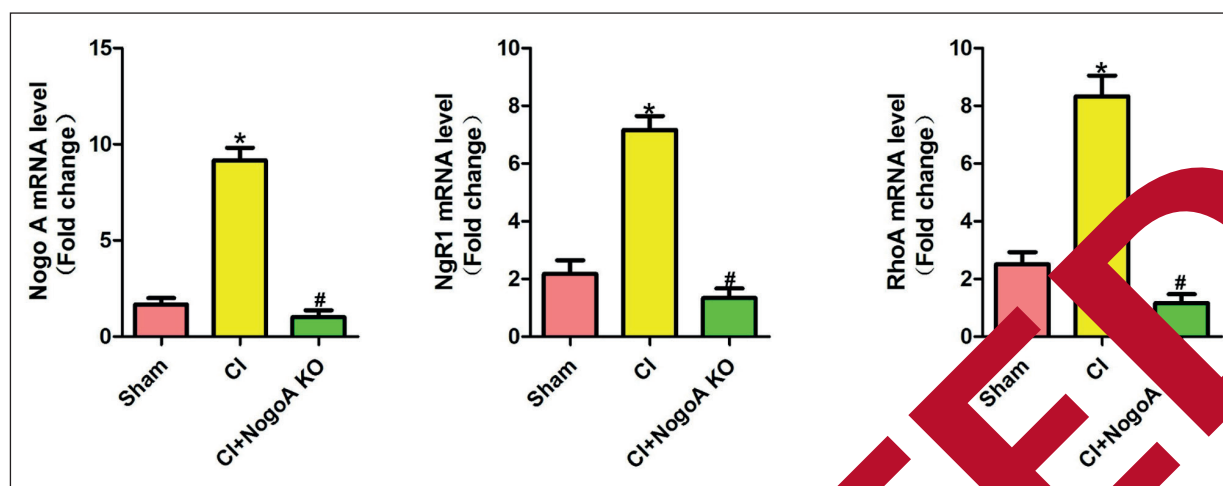


**Figure 1.** mRNA expression level of the NogoA/NgR1/RhoA signaling pathway in brain tissues of rats in each group. Sham operation group (Sham group), CI group and CI + NogoA gene KO group (CI+NogoA KO group). \* $p < 0.05$  vs. Sham group, showing a statistically significant difference. # $p < 0.05$  vs. CI group, showing a statistically significant difference.

cantly up-regulated when compared with Sham group ( $p < 0.05$ ). After NogoA gene was knocked out in rats, the mRNA expression levels of NogoA, NgR1, and RhoA in brain tissues were remarkably inhibited ( $p < 0.05$ ). This indicated successful induction of the NogoA KO model in rats.

#### Protein Expression of the NogoA/NgR1/RhoA Signaling Pathway in Brain Tissues of Rats in Each Group

Western blotting results revealed that, compared with Sham group, the protein expression levels of NogoA, NgR1, and RhoA in rats in CI group were markedly elevated ( $p < 0.05$ ), whereas were significantly reduced in CI+NogoA KO group ( $p < 0.05$ ) (Figure 3). The above results were consistent with the findings at the mRNA level. After the occurrence of CI, the expression levels of NogoA, NgR1, and RhoA in the infarction area of brain tissues of rats increased significantly.

#### Effect of NogoA KO on CI Area in Experimental Rats

After TTC staining, gray-white CI area appeared in brain tissues in the non-infarction area stained red. TTC staining results (Figure 4) indicated that no evident infarction area was observed in brain tissues of rats in Sham group. However, clear CI appeared in CI group. Meanwhile, certain infarction area appeared in brain tissues of rats in CI + NogoA KO group, which was markedly smaller than that of CI group ( $p < 0.05$ ). The above results indicated that inhib-

iting the NogoA/NgR1/RhoA signaling pathway could alleviate CI caused by middle cerebral artery ischemia to some extent.

#### H&E Staining Results of Brain Tissues of Rats in Each Group

Compared with CI group, rats in Sham group and CI+NogoA KO group showed the relatively complete structure of the hippocampus, as well as light and uniform cytoplasm. However, the structural integrity of neurons in brain tissues of rats in CI group disappeared. Furthermore, evident pathological changes appeared, such as edema, nuclear shift, and cell necrosis (Figure 4).

#### Nissl Staining Results in CI Area of Rats in Each Group

As shown in Figure 5, Nissl's body in brain tissues of rats in each group was stained. The results found that the number of Nissl's body in the three groups of rats was ( $62.33 \pm 2.93$ ) vs. ( $18.39 \pm 1.93$ ) vs. ( $55.34 \pm 2.91$ ), respectively, showing statistically significant differences ( $p < 0.05$ ). This suggested that inhibiting NogoA/NgR1/RhoA signals could effectively suppress CI-induced reduction of Nissl's body.

#### TUNEL Staining Results of Neurons in the Hippocampus of Rats in Each Group

TUNEL staining (Figure 6) illustrated that the positive rates of TUNEL were ( $2.49 \pm 1.23$ )%, ( $639.51 \pm 3.66$ )% and ( $20.67 \pm 2.96$ )% in the three groups, respectively ( $p < 0.05$ ). Moreover, Western



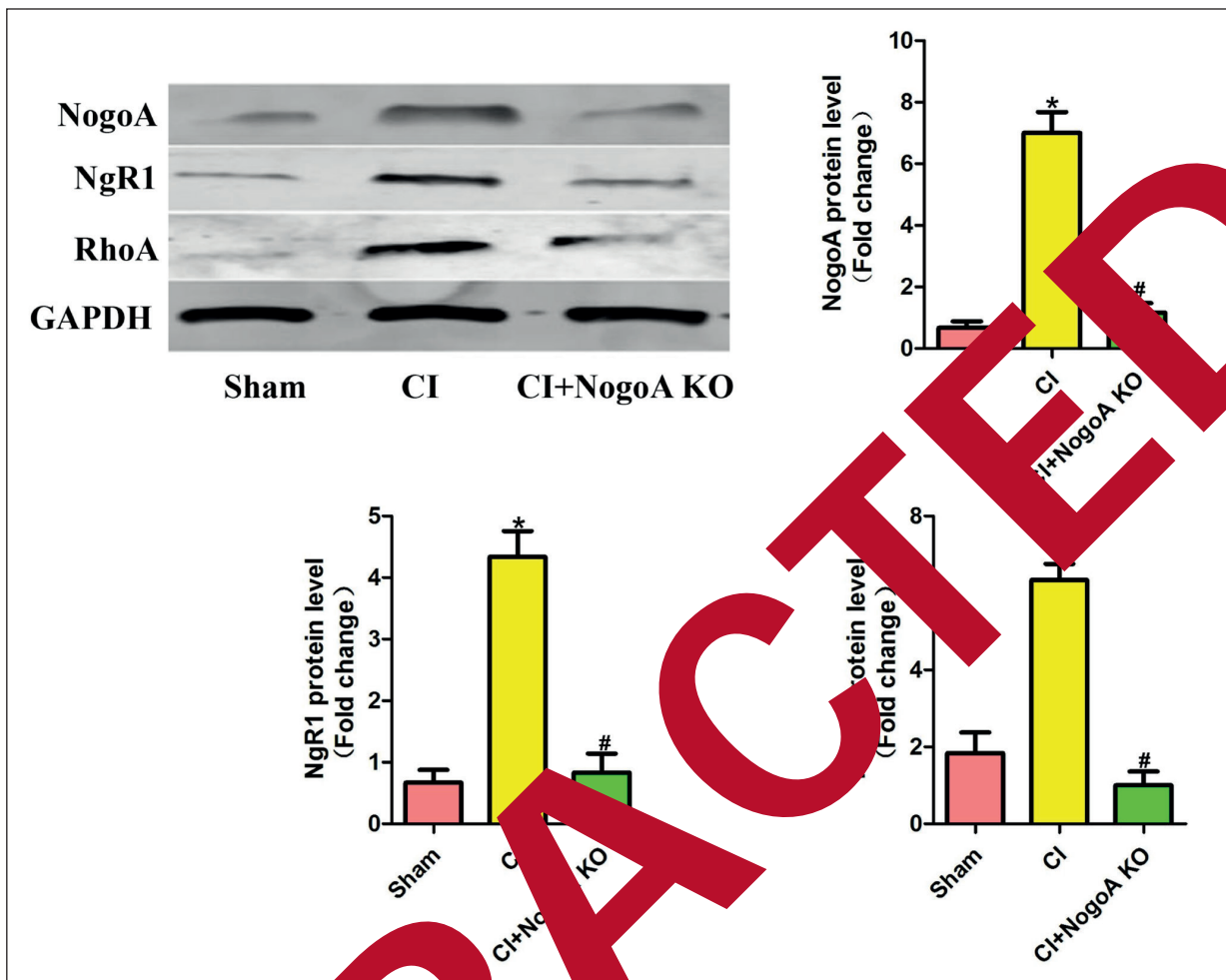


**Figure 2.** Protein expression level of the NogoA/NgR1/RhoA signaling pathway in brain tissues of rats in each group. Sham operation group (Sham group), CI group and NogoA gene KO group (CI+ NogoA KO group). # $p < 0.05$  vs. Sham group, displaying a statistically significant difference.

blotting demonstrated that the ratio of Bax/Bcl-2 in brain tissues of rats in the CI+NogoA KO group was significantly lower than that of CI group ( $p < 0.05$ ). The above results indicated that NogoA KO significantly reduced the apoptosis of neurons in the hippocampus of rats with CI.

#### Effect of NogoA KO on the Expression of PDGF in Brain Tissues of Rats

Ultimately, the expression level of PDGF in brain tissues of rats in each group was detected by immunohistochemistry. The results manifested that, after the occurrence of CI, the expression of PDGF in brain tissues of the infarction area was significantly suppressed. However, NogoA KO could further up-regulate the level of PDGF ( $p < 0.05$ ) (Figure 7).

#### Discussion

At present, CI is one of the most common cerebrovascular diseases worldwide<sup>9</sup>. Statistics have reported that the morbidity and mortality rates of CI in European and American countries are increasing year by year, especially in the United States<sup>10</sup>. The occurrence and development of CI are closely correlated with genetic alterations. With the development of modern molecular biology and bioinformatics, an increasing number of genes, RNAs, and proteins have been proved to be involved in the occurrence and development of CI<sup>11</sup>. Current researches have indicated that the apoptosis of neurons exerts an important effect on cerebral ischemia-reperfusion injury. Meanwhile, the apoptosis level determines the de-

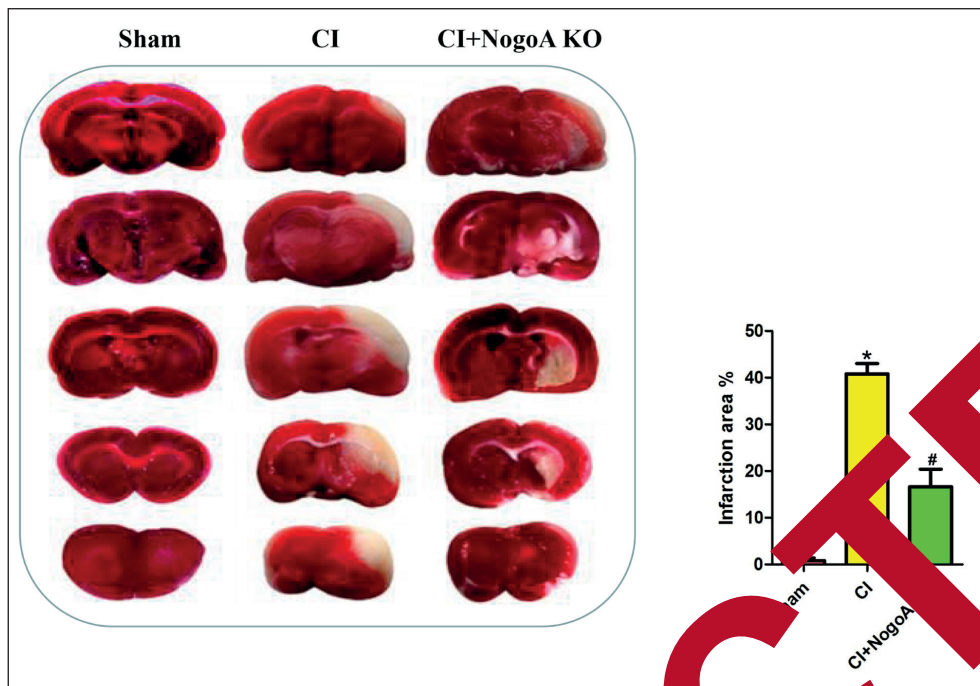


**Figure 3.** Effect of NogoA KO on CI area in experimental rats. Sham operation group (Sham group), CI group and CI + NogoA gene KO group (CI + NogoA KO group). # $p < 0.05$  vs. Sham group, displaying a statistically significant difference.

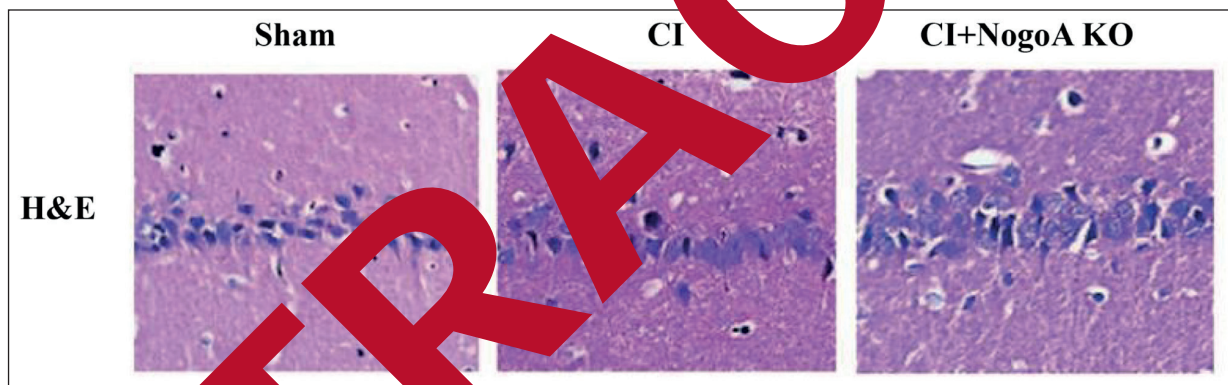


**Figure 4.** H&E staining results of brain tissues of rats in each group (200 $\times$ ). Sham operation group (Sham group), CI group and CI + NogoA gene KO group (CI + NogoA KO group).

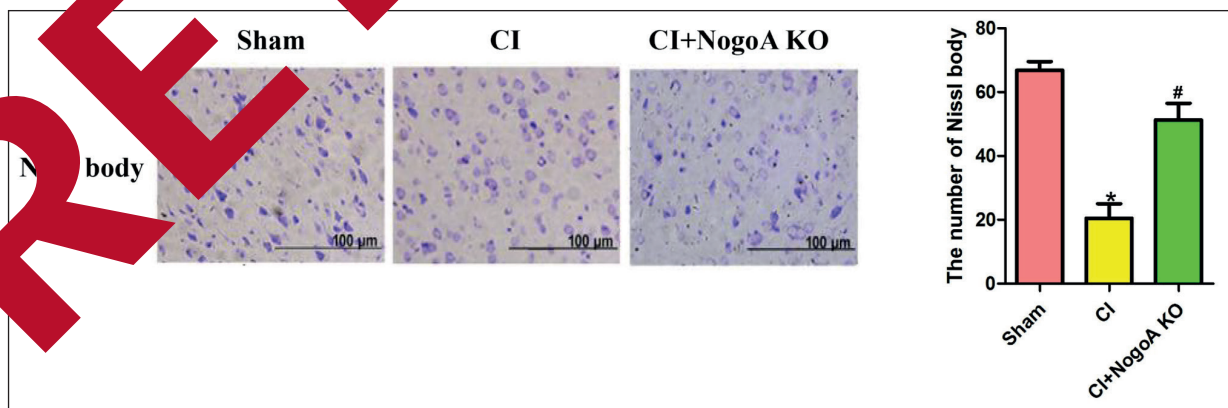


**Figure 5.** Nissl staining results in CI area of rats in each group (200 $\times$ ). Sham operation group (Sham group), CI group and CI + NogoA gene KO group (CI + NogoA KO group). # $p < 0.05$  vs. Sham group, with a statistically significant difference.

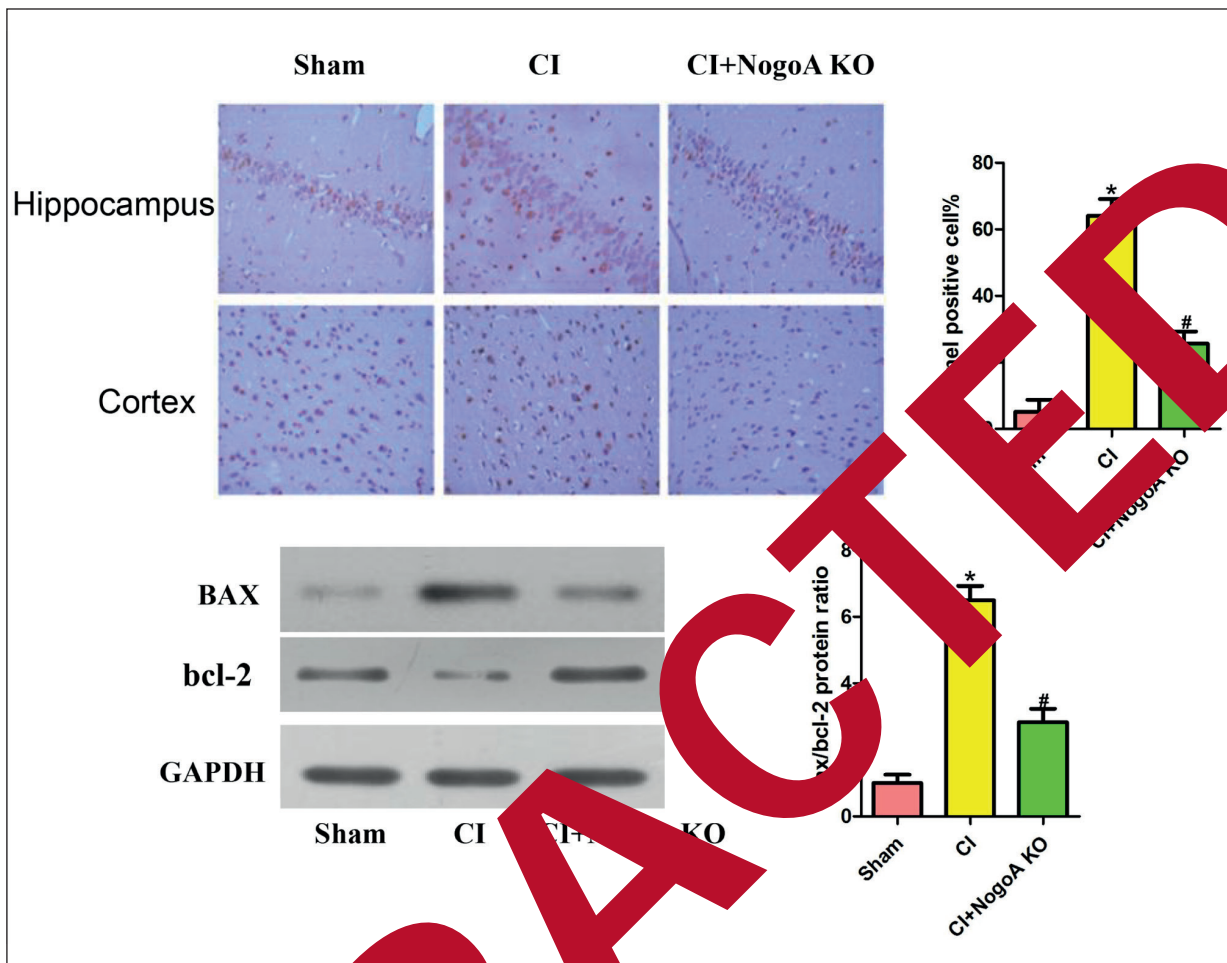


**Figure 6.** TUNEL staining results of neurons in the hippocampus of rats in each group (200×). Sham operation group (Sham group), CI group and CI + NogoA gene KO group (CI+ NogoA KO group). \* $p < 0.05$  vs. Sham group, with a statistically significant difference.

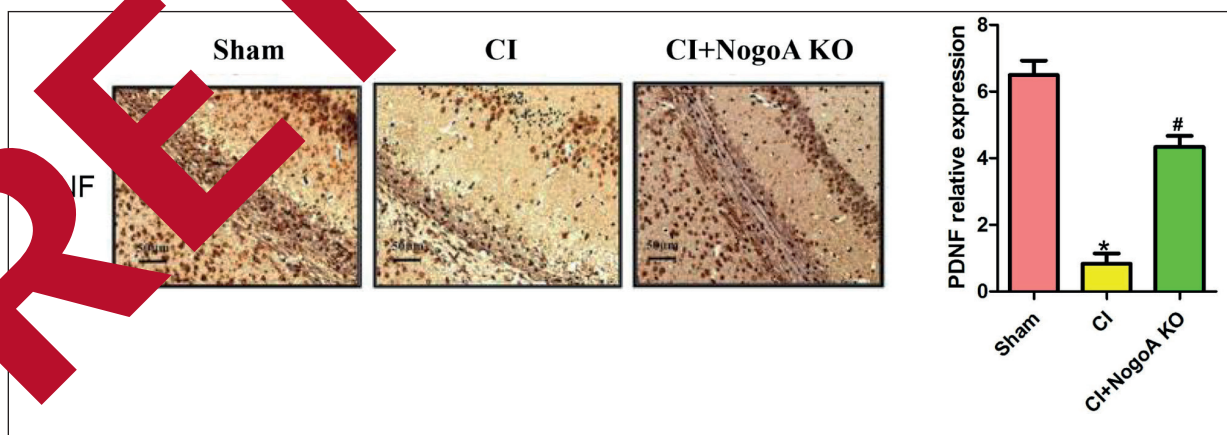


**Figure 7.** Effect of NogoA KO on the expression of PDGF in brain tissues of rats (400×). Sham operation group (Sham group), CI group and CI + NogoA gene KO group (CI+ NogoA KO group). \* $p < 0.05$  vs. Sham group, showing a statistically significant difference.



gree and prognosis of disease in a direct way<sup>12</sup>. In this study, the middle cerebral artery of SPF Wistar rats was embolized by a bolt from the carotid artery. This simulated the clinical onset process of CI much better than before. Meanwhile, NogoA was knocked out in rats, revealing the crucial role of NogoA in the occurrence and development of CI.

Apoptosis refers to programmed cell death controlled by genes under physiological or pathological conditions in order to maintain homeostasis<sup>13,14</sup>. In the process of CI, varying apoptosis-inducing signals are activated, thereby triggering edema, apoptosis or necrosis of neurons in the infarction area. In particular, during the first 6 h after CI, neuronal death is mainly manifested as necrosis. Subsequently, necrosis can be replaced by apoptosis. Hence, samples were collected at 48 h after CI in the present work. Meanwhile, the effect of NogoA KO on neuronal apoptosis in rats was further explored<sup>15,16</sup>. In the process of apoptosis, predominant expression levels of Bax and Bcl-2 determine the fate of cells in a direct way. Programmed cell death occurs when the expression of pro-apoptotic gene Bax dominates. However, apoptosis is inhibited when the expression of Bcl-2 is up-regulated<sup>17,18</sup>. In this study, NogoA KO notably increased the level of anti-apoptotic gene Bcl-2 and inhibited the level of pro-apoptosis gene Bax, thereby suppressing the results from ischemia and hypoxia.

Previous studies have reported that NogoA shows a predominant expression in hippocampus and cerebral cortex of mammals. Moreover, it exerts a protective effect on the repair of nervous system injury as well. Zemmar et al<sup>5</sup> have demonstrated that NogoA expressed in adult hippocampus exhibits a unique role in rapidly limiting physiological synaptic plasticity<sup>19</sup>. In addition, Deleute et al<sup>20</sup> have found that NogoA can be regarded as an important negative regulator for functional and structural plasticity in mature neuronal networks.

## Conclusions

Our findings demonstrate for the first time that the NogoA/NgR1/RhoA signaling pathway plays a crucial role in CI in rats. Furthermore, inhibiting the NogoA expression could effectively alleviate CI-induced brain injury and the apoptosis of neurons in rats.

## Conflict of Interests

The authors declare that they have no conflict of interest.

## References

- 1) XIA M, YE Z, SHI Y, ZHOU L, HUA Y. NogoA improves diabetes mellitus-associated cerebral infarction by increasing the expression of GLUT1 and GLUT3. *Mol Med Rep* 2018; 17: 1963-1969.
- 2) LIANG Y, CHEN J, ZHENG X, CHEN Z, LIU S, FANG X. Ultrasound-mediated lipidogen-mediated microbubble targeted therapy for acute cerebral infarction. *J Stroke Cerebrovasc Dis* 2018; 27: 686-696.
- 3) ZHU A, SHEN L, XIA L, CHEN Y, WANG Y. Wnt5a mediates chronic inter-thoracic pain by regulating non-canonical pathways, nerve regeneration, and inflammatory cytokines. *Cell Signal* 2018; 44: 51-61.
- 4) ZHANG M, ZHOU Y, HUO Y, NGUYEN T, ROSENBLATT MI, GUAQUIU VH. Semaphorin3A induces nerve regeneration in the adult corticospinal tract. *PLoS One* 2018; 13: e191962.
- 5) ZEMMAR A, CHEN CC, WEINMANN O, KAST B, VAJDA F, BOZEMAN J, MAAD N, ZUO Y, SCHWAB ME. Oligodendrocyte- and neuron-specific Nogo-A restrict dendritic branching and spine density in the adult mouse motor cortex. *Cereb Cortex* 2018; 28: 2103-2117.
- 6) BERRY S, WEINMANN O, FRITZ AK, RUST R, WOLFER D, SCHWAB ME, GERBER U, STER J. Loss of Nogo-A, mediated by the schizophrenia risk gene *Rtn4*, reduces mGlu3 expression and causes hyperexcitability in hippocampal CA3 circuits. *PLoS One* 2018; 13: e200896.
- 7) FARRER RG, KARTJE GL. Nogo-A interacts with TrkA to alter nerve growth factor signaling in Nogo-A-overexpressing PC12 cells. *Cell Signal* 2018; 44: 20-27.
- 8) SMEDFORS G, OLSON L, KARLSSON TE. A Nogo-like signaling perspective from birth to adulthood and in old age: brain expression patterns of ligands, receptors and modulators. *Front Mol Neurosci* 2018; 11: 42.
- 9) BONG JB, KANG HG, CHOO IS. Acute cerebral infarction after pyrethroid ingestion. *Geriatr Gerontol Int* 2017; 17: 510-511.
- 10) DONG XL, XU SJ, ZHANG L, ZHANG XO, LIU T, GAO QY, QIAN QQ, SUN BL, YANG MF. Serum resistin levels may contribute to an increased risk of acute cerebral infarction. *Mol Neurobiol* 2017; 54: 1919-1926.
- 11) HE X, LI DR, CUI C, WEN LJ. Clinical significance of serum MCP-1 and VE-cadherin levels in patients with acute cerebral infarction. *Eur Rev Med Pharmacol Sci* 2017; 21: 804-808.
- 12) QI X, SHAO M, SUN H, SHEN Y, MENG D, HUO W. Long non-coding RNA SNHG14 promotes microglia activation by regulating miR-145-5p/PLA2G4A in cerebral infarction. *Neuroscience* 2017; 348: 98-106.
- 13) ASHKENAZI A, FAIRBROTHER WJ, LEVERSON JD, SOUERS AJ. From basic apoptosis discoveries to advanced selective BCL-2 family inhibitors. *Nat Rev Drug Discov* 2017; 16: 273-284.



- 14) BAAR MP, BRANDT R, PUTAVET DA, KLEIN J, DERKS K, BOURGEOIS B, STRYECK S, RIJXEN Y, VAN WILLIGENBURG H, FEUTEL DA, VAN DER PLUIJM I, ESSERS J, VAN CAPPELLEN WA, VAN IJCKEN WF, HOUTSMULLER AB, POTHOF J, DE BRUIN R, MADL T, HOEIJMAKERS J, CAMPISI J, DE KEIZER P. Targeted apoptosis of senescent cells restores tissue homeostasis in response to chemotoxicity and aging. *Cell* 2017; 169: 132-147.
- 15) CHANG Y, HUANG W, SUN Q, LI S, YAN Z, WANG Q, LIU X. MicroRNA634 alters nerve apoptosis via the PI3K/Akt pathway in cerebral infarction. *Int J Mol Med* 2018; 42: 2145-2154.
- 16) SUZUKI M, TABUCHI M, IKEDA M, TOMITA T. Concurrent formation of peroxynitrite with the expression of inducible nitric oxide synthase in the brain during middle cerebral artery occlusion and reperfusion in rats. *Brain Res* 2002; 951: 113-120.
- 17) RENAULT TT, DEJEAN LM, MANON S. A brewing understanding of the regulation of Bax function by Bcl-xL and Bcl-2. *Mech Ageing Dev* 2017; 161: 201-210.
- 18) RUSSO A, CARDILE V, GRAZIANO A, AVOLA R, BRUNO M, RIGANO D. Involvement of Bax and Bcl-2 in induction of apoptosis by essential oils of three lebanese salvia species in human prostatic cancer cells. *Int J Mol Sci* 2018; 19: 292.
- 19) KUCHER K, JOHNS D, MAIER D, ABEL R, BADIERI C, BARON H, THIETJE R, CASHA S, MEINDL R, GOMEZ-MORAN B, PFISTER C, RUPP R, WEIDNER N, MIR A, SCHWAB ME, WISLA A. First-in-man intrathecal application of neurite growth promoting anti-Nogo-A antibodies in acute spinal cord injury. *Neurorehabil Neural Repair* 2018; 32: 578-587.
- 20) DELEKATE A, ZAGREBELSKA M, KRAMER S, SCHWAB ME, KORTE M. NogoA restricts synaptic plasticity in the adult hippocampus on a systems scale. *Proc Natl Acad Sci U S A* 2011; 108: 2569-2574.

**RETRACTED**